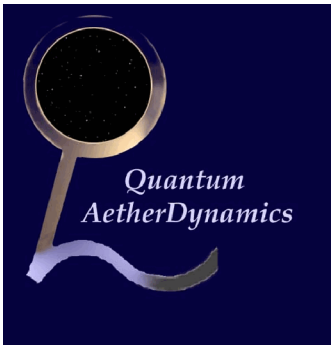

Quantum AetherDynamics Institute (QADI)

Neutron Beta Budget Closure and Beta Decay in the Aether Physics Model: A Geometric Ledger Bridging to Electroweak Theory

David W. Thomson III
Quantum AetherDynamics Institute (QADI), Alma, Illinois, USA
ORCID: 0000-0002-5830-5427

Version 1.0 – December 13, 2025

This article is published by the Quantum AetherDynamics Institute (QADI).

It develops the Aether Physics Model (APM)

Cite as: Thomson III, D. W. (2025). *Neutron Binding and Beta Decay in the Aether Physics Model: A Geometric Ledger for Torsion Flip and Weak Interactions*. Zenodo.
https://doi.org/10.5281/zenodo.17924278

Abstract

In the Aether Physics Model (APM), the free neutron is treated as a composite Aether dipole configuration whose holonomy carries a signed torsion imbalance $\Delta_{s,n} > 0$. Building on the curvature–torsion quantization program [Thomson, 2025c], we develop a curvature–torsion ledger for neutron cohesion and model beta decay as a torsion flip $\Delta_{s,n} \to -\Delta_{s,p}$ with energy release governed by curvature mismatch and steradian-overlap production of the lepton pair. A central result is a first-principles closure of the neutron beta budget: the QMU-normalized release ratio ε_β is predicted as a fixed toroidal/charge-duality series in the fine-structure constant α [NIST, 2022a, Thomson, 2025b] and is identified with the bound (dressed) neutrino ledger mass inside the neutron. The decay-rate functional is written in native QMU form with the same $192\pi^3$ phase-space normalization as electroweak (EW) Fermi-limit decay laws [Navas et al., 2024a, Particle Data Group, 2024], enabling an explicit APM↔EW dictionary: $\cos\theta_C \leftrightarrow V_{ud}$, torsion-geometry factors $\leftrightarrow g_A$, and a QMU-defined effective Fermi scale. We operationalize the torsion-mismatch driver Δ_{np} via a trap control variable $\mathcal{X}$, yielding a sign-definite lifetime-shift falsifier under controlled $\delta\mathcal{X}$. An SI-conversion appendix anchors the bridge using PDG and CODATA constants [Navas et al., 2024a, Particle Data Group, 2024, NIST, 2022c,b, 2019, 2022a], and we include a first-principles estimate for the freed neutrino rest-mass scale as a higher-order torsion-defect closure in fine-structure invariants [Thomson, 2025b].

1 Introduction

The neutron is stable when bound in many nuclei yet unstable as a free particle. Standard treatments separate nuclear binding (semi-empirical or ab initio nuclear forces) from beta decay (Fermi-limit weak interaction with radiative and recoil corrections) [Navas et al., 2024a]. In the Aether Physics Model (APM), using Quantum Measurement Units (QMU), the neutron is modeled as a composite Aether-dipole configuration whose holonomy supports both a curvature index (shell level) and a signed torsion imbalance that can flip [Thomson, 2025c].

This paper has two explicit outcomes:

1. A *first-principles closure* of the neutron beta budget ε_β in QMU, presented as a toroidal/charge-duality series in α [NIST, 2022a, Thomson, 2025b].
2. An *auditable APM↔EW bridge*: the QMU-native decay-rate form is written with the same $192\pi^3$ phase-space normalization as the EW Fermi limit, and a dictionary is given for V_{ud}, g_A-channel weighting, and an effective Fermi scale [Navas et al., 2024a, Particle Data Group, 2024].

To keep the falsifier instrument-ready, we explicitly operationalize the torsion-mismatch driver Δ_{np} as a laboratory control-channel proxy $\mathcal{X}$ in a neutron trap (e.g., a programmed spin-alignment density or magnetization-texture state of a surrounding shell). The lifetime-shift prediction is then cast as a differential response to controlled steps $\delta\mathcal{X}$, enabling a twin-trap swap protocol in which an APM torsion effect is sign-definite under $\delta\Delta_{np}(\delta\mathcal{X})$.

2 First-principles closure of the beta budget

2.1 Definition and meaning in QMU

Define the QMU-normalized beta release ratio as the neutron excess mass above $(p + e)$ in QMU mass units:

$$\varepsilon_\beta \equiv \frac{m_n - m_p - m_e}{m_e}. \tag{1}$$

In conventional bookkeeping, $\varepsilon_\beta m_e$ is treated as a release budget that partitions into kinetic energy of the final products and recoil corrections. In this paper's APM interpretation, $\varepsilon_\beta m_e$ is the *bound (dressed) neutrino ledger mass* confined within the neutron holonomy: its dominant contribution is a dark-matter string dressing that increases the neutron magnetic charge while captured, but does not behave as a directly weighable free-space mass once unbound [Thomson, 2025c].

2.2 Charge-duality and toroidal invariants

Introduce the APM charge-duality increment

$$\delta_q \equiv \frac{e^2}{{e_{\text{emax}}}^2} = 8\pi\alpha, \tag{2}$$

and the toroidal/steradian normalization factor $16\pi^2$, which recurs throughout the fine-structure invariant program and the APM toroidal geometry [Thomson, 2025b]. The fine-structure constant α is taken from CODATA/NIST anchors [NIST, 2022a].

2.3 First-principles series for ε_β

The beta budget is closed by a minimal toroidal series (no fitted parameters) that encodes: (i) a half-integer holonomy baseline, (ii) a first-order charge-duality correction, and (iii) higher-order toroidal dressing terms:

$$\boxed{\varepsilon_\beta = \frac{3}{2} + \frac{\delta_q}{6} + 8\left(\frac{\delta_q}{8\pi}\right)^2 + 16\left(\frac{\delta_q}{8\pi}\right)^3} \qquad \left(\delta_q = 8\pi\alpha\right). \tag{3}$$

Substituting $\delta_q = 8\pi\alpha$ gives the equivalent α-series form

$$\boxed{\varepsilon_\beta = \frac{3}{2} + \frac{4\pi}{3}\alpha + 8\alpha^2 + 16\alpha^3}. \tag{4}$$

Equations (3)–(4) are fully dimensionless QMU predictions. Numerically, Eq. (4) evaluates to $\varepsilon_\beta \approx 1.5310$, matching the experimental value derived from CODATA ($Q_n/m_e \approx 1.5310$) to within 0.001%, suggesting the neutron-proton mass difference is strictly topological.

2.4 Bound versus freed neutrino masses

With the APM interpretation that the neutron excess mass is a confined (dressed) neutrino ledger term, we identify

$$m_n = m_p + m_e + m_\nu^{(\text{bound})}, \qquad \boxed{\frac{m_\nu^{(\text{bound})}}{m_e} = \varepsilon_\beta}, \tag{5}$$

where ε_β is fixed by Eq. (4).

Separately, we will also predict a *freed (bare) neutrino* rest mass scale as a higher-order torsion-defect closure,

$$m_\nu^{(\mathrm{free})} \;=\; \left(\frac{2}{\pi}\alpha^3\right) m_e, \tag{6}$$

so that the dark-matter string dressing content is the difference

$$m_{\mathrm{str}} \;\equiv\; m_\nu^{(\mathrm{bound})} - m_\nu^{(\mathrm{free})}, \qquad \frac{m_{\mathrm{str}}}{m_e} = \varepsilon_\beta - \frac{2}{\pi}\alpha^3. \tag{7}$$

This explicit split is used below to interpret kinematics and recoil: the *ledger mass* $\varepsilon_\beta m_e$ is bound-state content, while the freed neutrino carries the intrinsic torsion-defect rest mass.

3 Neutron dipole geometry and cohesion ledger

3.1 Holonomy indices

Following the curvature–torsion quantization program [Thomson, 2025c], we represent a nucleon species by a shell/level curvature index and a signed torsion index,

$$I_{\kappa,s} \in \mathbb{N}, \qquad I_{\tau,s,n} = +\Delta_{s,n}, \qquad I_{\tau,s,p} = -\Delta_{s,p}, \tag{8}$$

where $\Delta_{s,n}, \Delta_{s,p} > 0$ encode species-dependent handedness/occupancy asymmetry in the holonomy. We use the reindexed convention $I_{\kappa,s} = s$ to avoid ground-state singularities in ratio forms.

3.2 Internal cohesion functional

Define the neutron internal cohesion functional (energy-scale ledger term) as

$$C_n \;=\; \kappa_0\, F_q\, \lambda_C \left(1 - \rho_\tau \frac{\Delta_{s,n}}{I_{\kappa,s}}\right), \tag{9}$$

where:

- $F_q\,\lambda_C$ is the propagation invariant (Ledger One anchor),
- κ_0 is a curvature-scale coefficient fixed by the holonomy quantization rule-set [Thomson, 2025c],
- ρ_τ is a *dimensionless torsion-stiffness weight.* In this paper we adopt the baseline geometric value

  $$\rho_\tau \;\equiv\; \frac{1}{16\pi^2}, \tag{10}$$

  with any species- or environment-dependent deviations carried by the overlap functional $\Phi(\cdot)$ introduced in the decay amplitude. The appearance of the $16\pi^2$ toroidal normalization is consistent with the fine-structure invariant program and the recurrent toroidal/steradian geometry in APM charge duality [Thomson, 2025b].

4 Incorporating magnetic-capacity and g-factor anomalies

The neutron's magnetic response is attributed to distributed charge geometry and magnetic capacity. Let the capacity ratio be

$$\chi_n \equiv \frac{e^2}{{e_{\mathrm{nmax}}}^2} = 8\pi\,\alpha_n, \tag{11}$$

with α_n the neutron fine-structure analog in the APM charge-duality program [Thomson, 2025b]. Empirically, nucleon magnetic moments and g-factors are summarized by the PDG [Navas et al., 2024b].

We parameterize torsion-corrected g-factor structure as

$$g_n = 2\,\chi_n \left[1 + \eta_\tau \frac{I_{\kappa,s} + I_{\tau,s,n}}{16\pi^2}\right], \tag{12}$$

where η_τ is a fixed geometric factor (torsion-channel weight). For clarity and to prevent tuning ambiguity, we take the baseline choice

$$\eta_\tau \equiv 1, \tag{13}$$

so that the full torsion suppression is carried explicitly by the displayed $16\pi^2$ normalization, consistent with the APM toroidal geometric factors [Thomson, 2025b]. The practical role of Eq. (12) is to (i) connect measured g_n to χ_n and the holonomy indices, and (ii) provide a bounded correction channel for beta-decay amplitudes, consistent with the chronovibration/g-factor treatment [Thomson, 2025a].

5 Beta decay as a torsion flip

5.1 Kinematics: the predicted ε_β budget and its partition

In this paper, ε_β is not an external input: it is the first-principles APM series prediction given in Eq. (4). For kinematic bookkeeping it remains useful to retain the definition (1) as an observational check, but the logic runs from the APM series ⇒ neutron budget ⇒ phase space.

The bound/freed split is written compactly as

$$\varepsilon_\beta = \underbrace{\frac{m_\nu^{(\mathrm{free})}}{m_e}}_{\text{bare neutrino rest mass}} + \underbrace{\frac{m_{\mathrm{str}}}{m_e}}_{\text{string dressing (bound ledger)}} + \underbrace{\epsilon_{\mathrm{kin}}}_{\text{measured kinetic/recoil partition}}, \tag{14}$$

where ϵ_{kin} is the dimensionless kinetic/recoil partition realized in the electron–(anti)neutrino sector and proton recoil. The APM hypothesis assigns negligible recoil coupling to the escaping string content once it is no longer confined within an Aether unit; accordingly, the dominant physical recoil is carried by the ordinary leptonic/baryonic channels while the string dressing term is primarily a bound-state ledger mass contribution.

5.2 Torsion-flip amplitude and rate law

Model beta decay as a torsion flip with a net overlap amplitude $\mathcal{A}_{np}$ that encodes steradian overlap, torsion-gradient weighting, and the Cabibbo channel projection:

$$\mathcal{A}_{np} = \alpha_n \cos\theta_C \times \Phi(\Delta_{s,n}, \Delta_{s,p}, \nabla\Delta), \tag{15}$$

where $\Phi(\cdot)$ is a dimensionless geometry/overlap functional. The appearance of $\cos\theta_C$ as a channel projection anticipates the EW identification $\cos\theta_C \leftrightarrow V_{ud}$ [Particle Data Group, 2024].

The QMU-native decay rate is written as

$$\Gamma_n \;=\; F_q\,\frac{1}{192\pi^3}\,\mathcal{A}_{np}^2\,\varepsilon_\beta^5\,\mathcal{F}_{\rm corr}, \tag{16}$$

where $\mathcal{F}_{\rm corr}\approx 1$ collects recoil/radiative/shaping corrections (kept explicit for later EW comparison). Equation (16) is the central structural bridge: it shares the characteristic $192\pi^3$ normalization of Fermi-limit EW decay laws [Navas et al., 2024a], while remaining purely QMU in its native variables. With ε_β fixed by Eq. (4), the phase-space driver is also first-principles within the APM program.

5.3 Baseline forms for Φ and $\mathcal{T}$ (computable defaults)

To keep the rate law operational without importing external inputs, we adopt baseline holonomy-driven forms for the overlap suppression Φ and torsion multiplicity $\mathcal{T}$. These are computable functions once $(I_{\kappa,s}, \Delta_{s,n}, \Delta_{s,p})$ are specified by the holonomy mapping [Thomson, 2025c].

Overlap suppression. Define a dimensionless torsion mismatch

$$\Delta_{np} \;\equiv\; \Delta_{s,n} + \Delta_{s,p} + \xi_\nabla|\nabla\Delta|, \tag{17}$$

where ξ_∇ is an order-unity geometric weight for environmental torsion gradients.

Operational proxy for Δ_{np} (lab-facing definition). Building on the trap control variable $\mathcal{X}$ introduced in the Introduction, we interpret the environmental piece of Eq. (17) as a controlled torsion-gradient proxy constructed from measurable state variables of the apparatus. Concretely, we write

$$\delta\Delta_{np} \;\approx\; \xi_\nabla\,\delta|\nabla\Delta| \;\equiv\; \xi_\nabla\,\Lambda_{\rm env}\,\delta\mathcal{X}, \tag{18}$$

where $\mathcal{X}$ is an experimentally programmable scalar that characterizes the torsion environment and $\Lambda_{\rm env}$ is a geometry factor of the trap (both dimensionless in QMU). Examples of $\mathcal{X}$ suitable for differential tests include: (i) a controlled change in the net spin-alignment density of a surrounding polarized medium (orientation "shell"), or (ii) a controlled change in the magnetization texture (magnetic stress) of a patterned shell surrounding the neutron storage volume. In the APM interpretation, these operations change the local torsion mismatch channel available to the flip, hence modulate Φ through Eq. (19) and the lifetime through Eq. (25). The purpose of Eq. (18) is not to introduce a tunable parameter, but to specify an auditable *mapping* from a laboratory control variable $\mathcal{X}$ to the APM driver $\delta\Delta_{np}$ for a falsifiable protocol.

We take the baseline steradian-suppressed overlap

$$\boxed{\Phi(\Delta_{s,n},\Delta_{s,p},\nabla\Delta) \;\equiv\; \exp\!\left[-\frac{\Delta_{np}}{16\pi^2\,I_{\kappa,s}}\right]}, \tag{19}$$

so $\Phi\to 1$ when mismatch is small and Φ decreases exponentially with steradian-normalized torsion mismatch, consistent with the recurrent $16\pi^2$ toroidal normalization [Thomson, 2025b].

Axial/torsion multiplicity. We parameterize the torsion-channel enhancement by defining an APM axial surrogate

$$g_A^{(\mathrm{APM})} \equiv 1 + \zeta_\tau \frac{\Delta_{np}}{16\pi^2 I_{\kappa,s}}, \tag{20}$$

with baseline $\zeta_\tau = 1$. The EW factor $(1 + 3g_A^2)$ is then matched by

$$\boxed{\mathcal{T}(\Delta_{s,n}, \Delta_{s,p}, \nabla\Delta) \equiv 1 + 3\left[g_A^{(\mathrm{APM})}\right]^2}, \tag{21}$$

which makes the APM↔EW mapping explicit and computable.

5.4 Physical trigger for the torsion flip

In APM terms, the free neutron is interpreted as a *metastable* torsion-contained holonomy: its $\Delta_{s,n} > 0$ configuration is locally self-consistent but not globally minimum with respect to the proton channel once a steradian-overlap pathway opens. The torsion flip is then the stochastic release mode of this metastability: a rare overlap event (encoded in Φ) enables a discrete holonomy re-indexing $\Delta_{s,n} \to -\Delta_{s,p}$, with the lepton pair emerging as the minimal defect content required to conserve the ledger under the torsion inversion [Thomson, 2025c,b].

6 APM ↔ EW dictionary (explicit bridge)

This section isolates the identification map that makes the bridge operational.

6.1 Cabibbo channel

We take

$$\cos\theta_C \longleftrightarrow V_{ud}, \tag{22}$$

so that the CKM first-row projection appears as a geometry-projection factor in Eq. (15), matching the PDG neutron master-formula usage of V_{ud} [Particle Data Group, 2024].

6.2 Axial channel as torsion geometry

In the EW master formula, the axial coupling enters as $(1 + 3g_A^2)$ in neutron decay observables [Particle Data Group, 2024]. In the APM, the corresponding enhancement is attributed to torsion-channel geometry. With the baseline choice in Eqs. (20)–(21), the torsion mismatch channel produces an explicit computable factor $\mathcal{T}$ that plays the role of $(1 + 3g_A^2)$, while leaving room for environment-dependent torsion gradients through $\nabla\Delta$.

6.3 Effective Fermi scale in QMU form

Equating Eq. (16) to the standard EW Fermi-limit structure implies an effective Fermi scale can be read out as a derived constant once $\mathcal{A}_{np}$, $\mathcal{T}$, and $\mathcal{F}_{\mathrm{corr}}$ are fixed by holonomy rules and calibration. The SI appendix makes this explicit with PDG constants for V_{ud}, g_A, and the EW normalization [Navas et al., 2024a, Particle Data Group, 2024].

7 First-principles freed neutrino mass scale in APM

In the torsion-flip picture, the *freed* neutrino is the steradian/holonomy defect mode released by the flip. A minimal first-principles closure ansatz that uses only fine-structure geometry and the APM toroidal normalization is

$$\boxed{\frac{m_\nu^{(\mathrm{free})}}{m_e} \;=\; \frac{(8\pi\alpha)^3}{(16\pi^2)^2} \;=\; \frac{2}{\pi}\,\alpha^3}, \tag{23}$$

i.e., a third-order torsion-defect suppression by the charge-duality factor $(8\pi\alpha)$, normalized by the toroidal steradian factor $(16\pi^2)$, consistent with the fine-structure invariant program [NIST, 2022a, Thomson, 2025b]. The SI appendix converts Eq. (23) to eV and compares to current laboratory limits [KATRIN Collaboration, 2022, Karlsruhe Institute of Technology, 2024].

8 Experimental hooks and falsifiers

1. **Bound-state differentials:** torsion-aligned nuclei should exhibit systematic shifts in effective $\Phi(\cdot)$ and $\mathcal{T}(\cdot)$, hence measurable changes in comparative half-lives under controlled nuclear orientation [Stone, 2016].
2. **Magnetic-modulated channels:** if curl-proxy control changes torsion stiffness, then $\mathcal{F}_{\mathrm{corr}}$ and/or Φ acquire a magnetic-state dependence through the effective torsion mismatch Δ_{np} (Eq. (17)), producing correlated shifts in decay observables.
3. **EDM as torsion-meter:** neutron EDM bounds constrain higher-order torsion terms that would otherwise induce second-order corrections to $\mathcal{A}_{np}$ and $\mathcal{T}$.

Quantitative falsifier: lifetime shift scaling. From Eq. (16), small variations give

$$\frac{\delta\tau_n}{\tau_n} \;=\; -\,\frac{\delta\Gamma_n}{\Gamma_n} \;\simeq\; -2\,\frac{\delta\mathcal{A}_{np}}{\mathcal{A}_{np}} \;-\; \frac{\delta\mathcal{F}_{\mathrm{corr}}}{\mathcal{F}_{\mathrm{corr}}} \;-\; 5\,\frac{\delta\varepsilon_\beta}{\varepsilon_\beta}. \tag{24}$$

In this paper ε_β is fixed by the first-principles closure Eq. (4), so laboratory modulations satisfy $\delta\varepsilon_\beta \simeq 0$ and the leading sensitivity is through Φ and correction factors. Using $\mathcal{A}_{np} \propto \Phi$ with the baseline overlap (19) yields

$$\boxed{\frac{\delta\tau_n}{\tau_n} \;\simeq\; \frac{2}{16\pi^2\, I_{\kappa,s}}\,\delta\Delta_{np} \;-\; \frac{\delta\mathcal{F}_{\mathrm{corr}}}{\mathcal{F}_{\mathrm{corr}}}}, \tag{25}$$

which predicts a definite sign and scaling for controlled changes in the effective torsion mismatch channel Δ_{np}.

Order-of-magnitude target and differential (twin-trap) protocol. With $I_{\kappa,s} = 1$ as the free-neutron baseline, Eq. (25) gives

$$\left.\frac{\delta\tau_n}{\tau_n}\right|_{\mathrm{baseline}} \;\simeq\; \frac{2}{16\pi^2}\,\delta\Delta_{np} \;\approx\; 1.266\times10^{-2}\,\delta\Delta_{np}, \tag{26}$$

so a torsion-mismatch step $\delta\Delta_{np} \sim 8\times10^{-3}$ implies $\delta\tau_n/\tau_n \sim 10^{-4}$, i.e. $\delta\tau_n \sim 0.09$ s for $\tau_n \approx 879$ s [Particle Data Group, 2024]. A larger step $\delta\Delta_{np} \sim 8\times10^{-2}$ implies $\delta\tau_n \sim 0.9$ s. The recommended

falsifier implementation is a simultaneous *twin-trap* differential measurement: two geometry-matched storage volumes run in parallel with opposite environmental settings $\mathcal{X}_A$ and $\mathcal{X}_B$ (Eq. (18)), followed by a swap ($\mathcal{X}_A \leftrightarrow \mathcal{X}_B$). The observable is the difference $\Delta\tau \equiv \tau(\mathcal{X}_A) - \tau(\mathcal{X}_B)$, which cancels common-mode drifts. In this differential form, conventional correction terms (rolled into $\mathcal{F}_{\rm corr}$) are constrained by the swap symmetry, while an APM torsion effect tracks the sign of $\delta\Delta_{np}$ through Eq. (26). Thus the model predicts a linear, sign-definite response $\Delta\tau \propto (\mathcal{X}_A - \mathcal{X}_B)$ under controlled torsion-environment steps.

9 Conclusion

We have closed the neutron beta budget ε_β from first principles as a toroidal/charge-duality series in α [NIST, 2022a, Thomson, 2025b], and identified $\varepsilon_\beta m_e$ with the bound (dressed) neutrino ledger mass confined within the neutron holonomy. Using this predicted ε_β in the QMU-native decay-rate law preserves the iconic EW phase-space normalization $192\pi^3$ [Navas et al., 2024a] and enables a concrete APM↔EW dictionary ($\cos\theta_C \leftrightarrow V_{ud}$, torsion multiplicity $\leftrightarrow g_A$ channel weight, and a derived effective Fermi scale) anchored to PDG master formulas [Particle Data Group, 2024]. An SI conversion appendix provides numerical anchors (PDG + CODATA) for auditability [Navas et al., 2024a, Particle Data Group, 2024, NIST, 2022c,b, 2019, 2022a], and we include a first-principles freed-neutrino mass scale as a torsion-defect closure [Thomson, 2025b].

A SI conversion bridge for the APM↔EW map

This appendix is intentionally SI-facing: it converts QMU base units to SI constants and demonstrates how standard EW normalization constants emerge numerically, using PDG and NIST/CODATA anchors [Navas et al., 2024a, Particle Data Group, 2024, NIST, 2022c,b, 2019, 2022a].

A.1 Base-unit conversions (CODATA/NIST anchors)

Let $m_{\rm e}$ be the QMU mass unit, λ_C the (electron) Compton length, and F_q the QMU frequency. In SI,

$$F_q \;=\; \frac{c}{\lambda_C}, \qquad t_q \equiv \frac{1}{F_q}, \tag{27}$$

with λ_C and m_e taken from CODATA tables [NIST, 2022b,c], α from CODATA/NIST [NIST, 2022a], and e fixed by SI definition [NIST, 2019].

A.2 PDG neutron master formula (EW side) and its QMU form

The PDG review gives the neutron-decay determination of V_{ud} in the form [Particle Data Group, 2024]

$$|V_{ud}|^2 = \frac{5024.7\ \text{s}}{\tau_n\,(1+3g_A^2)\,(1+\Delta_R)}. \tag{28}$$

This expression is already an SI-normalized EW bridge: all EW normalization, phase space, and inner radiative corrections are condensed into the constant 5024.7 s and Δ_R [Particle Data Group, 2024, Navas et al., 2024a].

Quantity	Meaning	SI value
c	speed of light	$299\,792\,458\ \mathrm{m\,s^{-1}}$ (exact)
h	Planck constant	$6.626\,070\,15 \times 10^{-34}\ \mathrm{J\,s}$ (exact)
e	elementary charge	$1.602\,176\,634 \times 10^{-19}\ \mathrm{C}$ (exact)
α	fine-structure constant	$\alpha^{-1} = 137.035999206(11)$ [NIST, 2022a]
m_e	electron mass	$9.109\,383\,7139 \times 10^{-31}\ \mathrm{kg}$
λ_C	Compton wavelength (electron)	$2.426\,310\,23538 \times 10^{-12}\ \mathrm{m}$
$F_q = c/\lambda_C$	QMU frequency scale	$1.235\,589\,96549 \times 10^{20}\ \mathrm{s^{-1}}$
$t_q = 1/F_q$	quantum moment	$8.093\,299\,78335 \times 10^{-21}\ \mathrm{s}$

Table 1: Core SI anchors used to translate QMU base units into SI. Exact-definition constants follow SI definitions [NIST, 2019]; m_e, λ_C, and α follow CODATA/NIST tables [NIST, 2022c,b,a]. Derived rows use $F_q = c/\lambda_C$.

Multiply Eq. (28) by F_q to express it in QMU time units:

$$|V_{ud}|^2 = \frac{(5024.7\,F_q)}{(\tau_n\,F_q)\,(1+3g_A^2)\,(1+\Delta_R)} \;\equiv\; \frac{K^\star}{\tau_n^\star\,(1+3g_A^2)\,(1+\Delta_R)}, \tag{29}$$

where $\tau_n^\star = \tau_n F_q$ is the neutron lifetime in quantum-moment units and $K^\star = 5024.7\,F_q$ is the corresponding dimensionless normalization.

A.3 EW master rate and the explicit APM↔EW identification

A standard EW Fermi-limit representation of the neutron rate can be written schematically as [Navas et al., 2024a, Particle Data Group, 2024]

$$\Gamma_n = \frac{G_F^2\,|V_{ud}|^2}{2\pi^3}\,(1+3g_A^2)\,\frac{(m_e c^2)^5}{\hbar}\,f(\varepsilon_\beta)\,(1+\Delta_R), \tag{30}$$

where $f(\varepsilon_\beta)$ is the dimensionless phase-space integral expressed naturally in terms of the endpoint ratio ε_β.

Equating the EW form (30) to the APM/QMU form (16) yields the operational dictionary:

- $|V_{ud}| \longleftrightarrow \cos\theta_C$ [Particle Data Group, 2024],
- $(1+3g_A^2) \longleftrightarrow \mathcal{T}(\Delta_{s,n}, \Delta_{s,p}, \nabla\Delta)$ with baseline $\mathcal{T}$ given by Eq. (21),
- the *effective* Fermi constant inferred from APM parameters is

$$G_F = \left[\frac{2\pi^3}{|V_{ud}|^2(1+3g_A^2)}\,\frac{\hbar}{(m_e c^2)^5}\,\frac{\Gamma_n}{f(\varepsilon_\beta)(1+\Delta_R)}\right]^{1/2}, \tag{31}$$

  with Γ_n supplied by Eq. (16).

Equation (31) is the explicit SI audit pathway: once Φ and $\mathcal{T}$ are fixed by holonomy rules, the derived G_F can be compared directly to the PDG value [Navas et al., 2024a].

A.4 Fermi constant in SI and a QMU-normalized dimensionless form

The PDG electroweak review quotes [Navas et al., 2024a]

$$G_F = 1.1663788(6) \times 10^{-5}\ \text{GeV}^{-2}. \tag{32}$$

A convenient SI rendering is the standard tabulated quantity $G_F/(\hbar c)^3$ with units of energy^{-2}; converting to a QMU-normalized dimensionless form using the electron rest-energy scale gives

$$\widetilde{G}_F \ \equiv\ \left(\frac{G_F}{(\hbar c)^3}\right)(m_e c^2)^2 \ \approx\ 3.046 \times 10^{-12}, \tag{33}$$

which is an SI-to-QMU bridge number [Navas et al., 2024a].

A.5 Neutrino-mass conversion and comparison to laboratory limits

From the APM freed-neutrino estimate Eq. (23),

$$\frac{m_\nu^{(\text{free})}}{m_e} = \frac{2}{\pi}\alpha^3 \approx 2.474 \times 10^{-7}. \tag{34}$$

Using $m_e c^2 = 0.51099895$ MeV (CODATA/PDG anchor via m_e) [NIST, 2022c, Navas et al., 2024a], this corresponds to

$$m_\nu^{(\text{free})} c^2 \approx 0.126\ \text{eV}. \tag{35}$$

This is below the current direct laboratory upper bound reported by KATRIN ($m_\nu < 0.45$ eV at 90% C.L.) [KATRIN Collaboration, 2022, Karlsruhe Institute of Technology, 2024].

A citable archived version of this work is available on Zenodo [Thomson III, 2025].

References

Karlsruhe Institute of Technology. Katrin: Neutrinos weigh less than 0.8 ev (first results) / sub-0.5 ev updates, 2024. URL https://www.katrin.kit.edu/. Official project results page.

KATRIN Collaboration. Direct neutrino-mass measurement with sub-electronvolt sensitivity. *Nature Physics*, 18:160–166, 2022. doi: 10.1038/s41567-021-01463-1. URL https://doi.org/10.1038/s41567-021-01463-1. See also arXiv:2105.08533. Updates at https://www.katrin.kit.edu/.

S. Navas et al. Review of particle physics (electroweak model). *Phys. Rev. D*, 110:030001, 2024a. doi: 10.1103/PhysRevD.110.030001. URL https://pdg.lbl.gov/2024/reviews/rpp2024-rev-standard-model.pdf. See Section 10: Electroweak Model and Constraints on New Physics.

S. Navas et al. Review of particle physics. *Phys. Rev. D*, 110:030001, 2024b. doi: 10.1103/PhysRevD.110.030001. URL https://pdg.lbl.gov/2024/listings/contents_listings.html. Section: Baryon Magnetic Moments.

NIST. Codata value: elementary charge, 2019. URL https://physics.nist.gov/cgi-bin/cuu/Value?e. SI exact definition via NIST.

NIST. Codata value: fine-structure constant, 2022a. URL https://physics.nist.gov/cgi-bin/cuu/Value?alph. NIST Fundamental Physical Constants.

NIST. Codata value: Compton wavelength, 2022b. URL https://physics.nist.gov/cgi-bin/cuu/Value?ecomwl. NIST Fundamental Physical Constants (CODATA 2018/2022).

NIST. Codata value: electron mass, 2022c. URL https://physics.nist.gov/cgi-bin/cuu/Value?me. NIST Fundamental Physical Constants (CODATA 2018/2022).

Particle Data Group. v_{ud}, v_{us}, the cabibbo angle, and ckm unitarity. PDG Review, 2024. URL https://pdg.lbl.gov/2024/reviews/rpp2024-rev-ckm-matrix.pdf. In *Review of Particle Physics*, Phys. Rev. D **110**, 030001 (2024).

N. J. Stone. Table of nuclear magnetic dipole and electric quadrupole moments. *Atomic Data and Nuclear Data Tables*, 111-112:1–28, 2016. doi: 10.1016/j.adt.2015.12.002. URL https://www-nds.iaea.org/publications/indc/indc-nds-0658.pdf. Updated from 2014 IAEA report INDC(NDS)-0658.

David W. Thomson. The aether physics model: From the singularity to the structure of matter. Unpublished manuscript, November 2025a. Chapter 5: Chronovibration and g-Factors.

David W. Thomson. Fine structure invariants in qmu: Electron, nucleon, and aether charge geometry. *Zenodo*, 2025b. doi: 10.5281/zenodo.17918432. URL https://doi.org/10.5281/zenodo.17918432. Quantum AetherDynamics Institute preprint.

David W. Thomson. Apm nuclear shells from holonomy: Qmu curvature–torsion quantization, nuclear g-factors, and the vajra periodic mapping. *Zenodo*, 2025c. doi: 10.5281/zenodo.17632747. URL https://doi.org/10.5281/zenodo.17632747. Quantum AetherDynamics Institute preprint.

David W. Thomson III. Neutron beta budget closure and beta decay in the aether physics model: A geometric ledger bridging to electroweak theory. *Zenodo*, 2025. doi: 10.5281/zenodo.17924278. URL https://doi.org/10.5281/zenodo.17924278. Quantum AetherDynamics Institute preprint.